FSI with Application in Hemodynamics
Analysis and Simulation

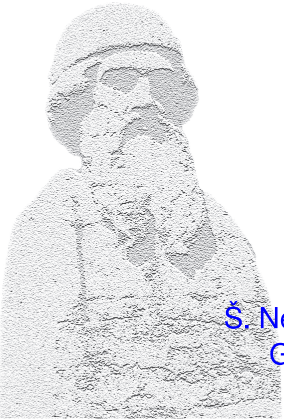

Mária Lukáčová

Institute of Mathematics, University of Mainz

A. Hundertmark (Uni-Mainz)
Š. Nečasová (Academy of Sciences, Prague)
G. Rusnáková (Uni-Košice/Uni-Mainz)

II. Numerical Modelling

Numerical schemes for the FSI problems

- strong coupled schemes (inner subiterations or fully composite schemes)
- weakly coupled schemes (no subiterations needed)

Numerical schemes for the FSI problems

- strong coupled schemes (inner subiterations or fully composite schemes)
- weakly coupled schemes (no subiterations needed)

- for aerodynamical problems: weakly coupled schemes: OK
- for biomechanical probelms: kind of stronger coupling, subiterations are typically needed

Numerical schemes for the FSI problems

- strong coupled schemes (inner subiterations or fully composite schemes)
- weakly coupled schemes (no subiterations needed)

- for aerodynamical problems: weakly coupled schemes: OK
- for biomechanical probelms: kind of stronger coupling, subiterations are typically needed

- many numerical approaches for the FSI: immersed boundary, Lagrangian, Arbitrary Eulerian-Lagrangian (ALE)

FSI for hemodynamical applications

1. Quarteroni, Formaggia, Veneziani, Nobile et al. ('01-'07) . . . inner subiterations

1. Quarteroni, Formaggia, Veneziani, Nobile et al. ('01-'07) ... inner subiterations
2. Hron, Turek et al. ('09) monolitic scheme (strong coupling)

FSI for hemodynamical applications

1. Quarteroni, Formaggia, Veneziani, Nobile et al. ('01-'07) ... inner subiterations
2. Hron, Turek et al. ('09) monolitic scheme (strong coupling)
3. Guidoboni, Glowinski, Cavallini, Čaniè ('09): weak coupling: kinematical coupling

FSI for hemodynamical applications

1. Quarteroni, Formaggia, Veneziani, Nobile et al. ('01-'07) . . . inner subiterations
2. Hron, Turek et al. ('09) monolitic scheme (strong coupling)
3. Guidoboni, Glowinski, Cavallini, Čaniċ ('09): weak coupling: kinematical coupling
4. Janela, Moura, Sequeira ('10): simulations for non-Newtonian FSI

FSI for hemodynamical applications

1. Quarteroni, Formaggia, Veneziani, Nobile et al. ('01-'07) . . . inner subiterations
2. Hron, Turek et al. ('09) monolitic scheme (strong coupling)
3. Guidoboni, Glowinski, Cavallini, Čaniċ ('09): weak coupling: kinematical coupling
4. Janela, Moura, Sequeira ('10): simulations for non-Newtonian FSI
5. Hundertmark, Lukáčová, Rusnáková ('08,'10, '11): analysis and simulations for non-Newtonian FSI schemes (global and kinematical coupling)

Outline

Discretization method

- Fluid equations
  - UG software toolbox

Discretization method

- **Fluid equations**
  - UG software toolbox
  - FV-type schemes

Discretization method

- Fluid equations
  - UG software toolbox
  - FV-type schemes
  - pseudo compressibility stabilization

Discretization method

- Fluid equations
  - UG software toolbox
  - FV-type schemes
  - pseudo compressibility stabilization
  - Newton/fixed point linearization of convective term

Discretization method

- Fluid equations
  - UG software toolbox
  - FV-type schemes
  - pseudo compressibility stabilization
  - Newton/fixed point linearization of convective term
- fixed point iterations of non-linear viscosity

$$\mu(|D(\nabla \boldsymbol{u})|)D(\nabla \boldsymbol{u}) \approx \mu(|D(\nabla \boldsymbol{u}^{old})|)D(\nabla \boldsymbol{u})$$

- Fluid equations
  - UG software toolbox
  - FV-type schemes
  - pseudo compressibility stabilization
  - Newton/fixed point linearization of convective term
- fixed point iterations of non-linear viscosity

$$\mu(|D(\nabla \boldsymbol{u})|)D(\nabla \boldsymbol{u}) \approx \mu(|D(\nabla \boldsymbol{u}^{old})|)D(\nabla \boldsymbol{u})$$

- **Structure equation**

$$\frac{\partial^2 \eta}{\partial t^2} - a\frac{\partial^2 \eta}{\partial x_1^2} + b(1/\eta)\eta - c\frac{\partial^3 \eta}{\partial x_1^2 \partial t} = RHS(u, p, R_0)$$

- finite difference method in time (Newmark scheme)
- finite difference method in space (central approximations)

. . . second order

Outline

Fluid-Structure Coupling 1

- I. Strong coupling - **global iteration method k=1,2, ...**
  - solve fluid eq. & structure eq. on the domain $\Omega(\eta^k)$ for t^n, $n = 1, 2, 3 \dots$
  - homogeneous Dirichlet or Neumann boundary conditions

Fluid-Structure Coupling 1

- I. Strong coupling - **global iteration method k=1,2, …**
  - solve fluid eq. & structure eq. on the domain $\Omega(\eta^k)$ for t^n, $n = 1, 2, 3 \ldots$
  - homogeneous Dirichlet or Neumann boundary conditions
- $(\xi = \partial_t \eta)$

$$\frac{\xi^{n+1} - \xi^n}{\Delta t} - a\alpha \frac{\partial^2 \eta^{n+1}}{\partial x_1^2} + b\alpha\eta^{n+1} - c\alpha \frac{\partial^2 \xi^{n+1}}{\partial x_1^2}$$

$$= RHS(p^n, u^n, R_0) + (1-\alpha)\left(a\frac{\partial^2 \eta^n}{\partial x_1^2} - b\eta^n + c\frac{\partial^2 \xi^n}{\partial x_1^2} \right)$$

$$\frac{\eta^{n+1} - \eta^n}{\Delta t} = \alpha\xi^{n+1} + (1-\alpha)\xi^n, \qquad \alpha = 0.5$$

Global iteration with respect to the domain

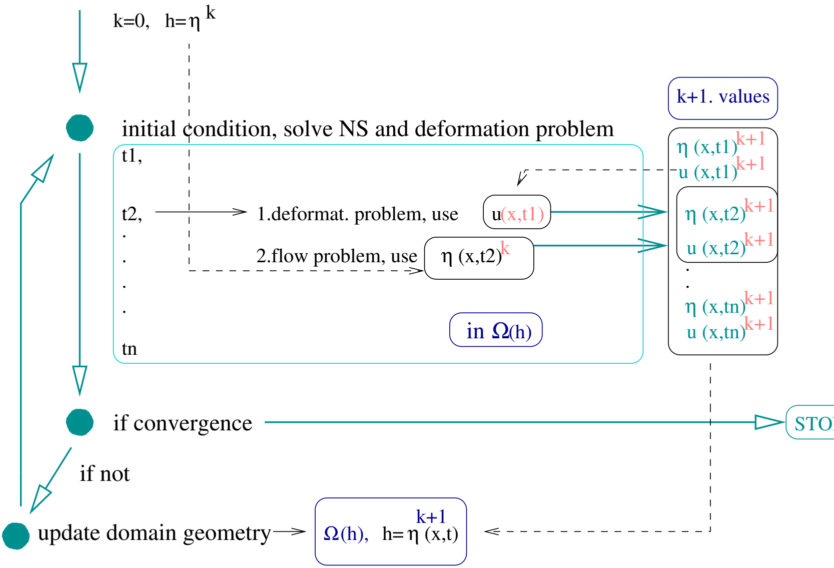

II. Kinematical coupling [Guidoboni et al. ('09)]

- solve Fluid eq. + Structure eq. on $\Omega(\eta^n)$ for $t \in [t^n, t^{n+1}]$
- **split structure eq.** into 2 parts
- kinematical lateral B.C.

$$u_2|_{y=H} = \frac{\partial \eta}{\partial t} = \xi$$

II. Kinematical coupling [Guidoboni et al. ('09)]

- solve Fluid eq. + Structure eq. on $\Omega(\eta^n)$ for $t \in [t^n, t^{n+1}]$
- **split structure eq.** into 2 parts
- kinematical lateral B.C.

$$u_2|_{y=H} = \frac{\partial \eta}{\partial t} = \xi$$

- **1. hydrodynamic part**
  fluid eq. + $\xi = u_2|_{y=H}$

$$\frac{\partial \xi}{\partial t} = c \frac{\partial^2 \xi}{\partial {x_1}^2} + RHS(u, p)$$

- **2. elastic part**

$$\frac{\partial \eta}{\partial t} = \xi$$

$$\frac{\partial \xi}{\partial t} = a \frac{\partial^2 \eta}{\partial {x_1}^2} - b(1/\eta)\eta + RHS(R_0)$$

- Kinematical coupling / Discretization

A operator: hydrodynamic part

Fluid solver +

$$\frac{\xi^{n+1/2} - \xi^n}{\Delta t} - c\alpha \frac{\partial^2 \xi^{n+1/2}}{\partial x_1^2} = RHS(p^n, u^n) + c(1-\alpha)\frac{\partial^2 \xi^n}{\partial x_1^2},$$

B operator: elastic part

$$\frac{\eta^{n+1} - \eta^n}{\Delta t} = \beta \xi^{n+1} + (1-\beta)\xi^{n+1/2}, \quad \beta = 0.5$$

$$\frac{\xi^{n+1} - \xi^{n+1/2}}{\Delta t} - a\alpha \frac{\partial^2 \eta^{n+1}}{\partial x_1^2} + b(1/\eta^n)\alpha \eta^{n+1}$$

$$= RHS(R_0) + a(1-\alpha)\frac{\partial^2 \eta^n}{\partial x_1^2} - b(1/\eta^n)(1-\alpha)\eta^n \quad \alpha = 1, 0.5$$

Types of splitting

- kinematical splitting scheme of the **Marchuk-Yanenko type**
  - 1st order accurate
  - $A_{\triangle t} \curvearrowright B_{\triangle t}$

    in the $(n+1)-\mathrm{th}$ time-step on $\Omega(t^n)$

Types of splitting

- kinematical splitting scheme of the **Marchuk-Yanenko type**
  - 1st order accurate
  - $A_{\triangle t} \curvearrowright B_{\triangle t}$
    in the $(n+1) - \mathrm{th}$ time-step on $\Omega(t^n)$
- kinematical splitting scheme of the **Strang-type kinematical splitting**
  - 2nd order accurate
  - $B_{\triangle t/2} \curvearrowright A_{\triangle t} \curvearrowright B_{\triangle t/2}$
    in the $(n+1) - \mathrm{th}$ time-step on $\Omega(t^n)$

Outline

Arbitrary Lagragian-Eulerian Mapping

$$\mathcal{A}_t : \Omega_0 \to \Omega_t$$

$$\mathcal{A}_t(\mathbf{X}) = \mathbf{x} \in \Omega_t$$

$$f(t, \boldsymbol{x}) \equiv \tilde{f}(t, \mathcal{A}_t^{-1}\boldsymbol{x}) \equiv \tilde{f}(t, \mathbf{X})$$

$\frac{\mathcal{D}^{\mathcal{A}}\boldsymbol{u}}{\mathcal{D}t}$ ALE derivative $\boldsymbol{w} := \frac{\partial \mathbf{x}}{\partial t}$ “grid velocity"

$$\frac{\mathcal{D}^{\mathcal{A}}\boldsymbol{u}(t, \boldsymbol{x})}{\mathcal{D}t} := \frac{\partial \tilde{\boldsymbol{u}}(t, \mathbf{X})}{\partial t}$$

$$= \frac{\partial \boldsymbol{u}(t, \boldsymbol{x})}{\partial t} + \boldsymbol{w} \cdot \nabla \boldsymbol{u}(t, \boldsymbol{x})$$

Weak formulation of coupled problem

- test functions: $\boldsymbol{v} \in V$, where

$$\boldsymbol{V} \equiv \left\{ \boldsymbol{v} \in W^{1,p}(\Omega(t))^2 : v_1|_{\Gamma_{wall}} = 0, v_2|_{x_2=0} = 0 \right\}$$

$\frac{\mathcal{D}^{\mathcal{A}}\boldsymbol{u}}{\mathcal{D}t}$ ALE derivative $\quad$ $\boldsymbol{w} := \frac{\partial \boldsymbol{x}}{\partial t}$ grid velocity

$$\frac{\mathcal{D}^{\mathcal{A}}\boldsymbol{u}}{\mathcal{D}t} := \frac{\partial \boldsymbol{u}}{\partial t} + \boldsymbol{w} \cdot \nabla \boldsymbol{u}(\boldsymbol{x}, t)$$

Weak formulation of coupled problem

- test functions: $\boldsymbol{v} \in V$, where

$$\boldsymbol{V} \equiv \left\{ \boldsymbol{v} \in W^{1,p}(\Omega(t))^2 : v_1|_{\Gamma_{wall}} = 0, v_2|_{x_2=0} = 0 \right\}$$

$\frac{\mathcal{D}^{\mathcal{A}}\boldsymbol{u}}{\mathcal{D}t}$ ALE derivative $\boldsymbol{w} := \frac{\partial \boldsymbol{X}}{\partial t}$ grid velocity

$$\frac{\mathcal{D}^{\mathcal{A}}\boldsymbol{u}}{\mathcal{D}t} := \frac{\partial \boldsymbol{u}}{\partial t} + \boldsymbol{w} \cdot \nabla \boldsymbol{u}(\boldsymbol{x}, t)$$

$$\int_{\Omega(t)} \frac{\mathcal{D}^{\mathcal{A}}\boldsymbol{u}}{\mathcal{D}t} \boldsymbol{v} \,\mathrm{d}\boldsymbol{x} + \int_{\Omega(t)} ((\boldsymbol{u} - \boldsymbol{w}) \cdot \triangledown \boldsymbol{u}) \boldsymbol{v} \mathrm{d}\boldsymbol{x} -$$
$$\int_{\Omega(t)} p \,\mathrm{div}\, \boldsymbol{v} \,\mathrm{d}\boldsymbol{x} + \frac{1}{\rho} \int_{\Omega(t)} 2\mu(|\mathbf{D}(\boldsymbol{u})|)\mathbf{D}(\boldsymbol{u}) : \mathbf{D}(\boldsymbol{v}) \,\mathrm{d}\boldsymbol{x} +$$
$$\int_0^L \left(\frac{\partial^2 \eta}{\partial t^2} + b\eta \right) v_2|_{\Gamma_{wall}} \mathrm{d}x_1 + \int_0^L \left(a\frac{\partial \eta}{\partial x_1} + c\frac{\partial^2 \eta}{\partial t\, \partial x_1} \right) \frac{\partial (v_2|_{\Gamma_{wall}}}{\partial x_1}$$
$$= \int_0^{R_0} P_{in} v_1|_{x_1=0} \mathrm{d}x_2, \quad \forall \boldsymbol{v} \in \boldsymbol{V},\ a.e.t \in I.$$

Energy estimates

- with G. Rusnáková
  - weak formulation of the semi-discrete coupled problem
    - $p \geq 2$
    - test with $\boldsymbol{u}^{n+1}$
    - kinematic pressure boundary conditions on infow / outflow
    - symmetry boundary conditions $x_2 = 0$

Outline

Energy estimate for $\xi^{n+1/2} := u_2^{n+1}|_{\Gamma_{wall}}$

$$\frac{1}{2}||\boldsymbol{u}^{n+1}||^2_{L^2(\Omega(t_{n+1}))} + \frac{c^*}{2\rho}\Delta t||\boldsymbol{u}^{n+1}||^2_{W^{1,2}(\Omega(t_{n+1/2}))}$$
$$+\frac{1}{2}||\xi^{n+\frac{1}{2}}||^2_{L^2(0,L)} + c\Delta t||\xi_x^{n+\frac{1}{2}}||^2_{L^2(0,L)} \leq$$
$$\leq \frac{1}{2}||\boldsymbol{u}^n||^2_{L^2(\Omega(t_n))} + \frac{1}{2}||\xi^n||^2_{L^2(0,L)} + c\Delta t|P_{in}^{n+1}|^2$$

- we obtain the following estimate for the A-operator

$$\begin{aligned} & ||\xi^{n+\frac{1}{2}}||^2_{L^2(0,L)} + ||\boldsymbol{u}^{n+1}||^2_{L^2(\Omega(t_{n+1}))} \\ \leq \quad & ||\xi^n||^2_{L^2(0,L)} + ||\boldsymbol{u}^n||^2_{L^2(\Omega(t_n))} + 2c\Delta t|P_{in}^{n+1}|^2 \end{aligned}$$

Outline

Energy of the solution

Energy of A-operator:

$$||\xi^{n+\frac{1}{2}}||^2_{L^2(0,L)} \leq ||\xi^n||^2_{L^2(0,L)} + ||\boldsymbol{u}^n||^2_{L^2(\Omega(t_n))} - ||\boldsymbol{u}^{n+1}||^2_{L^2(\Omega(t_{n+1}))}$$
$$+ \quad 2c\Delta t|P^{n+1}_{in}|^2$$

Energy of B-operator:

$$\begin{aligned} & a\,||\eta^{N+1}_{x_1}||^2_{L^2(0,L)} + b\,||\eta^{N+1}||^2_{L^2(0,L)} + ||\xi^{N+1}||^2_{L^2(0,L)} \\ = \quad & a\,||\eta^0_{x_1}||^2_{L^2(0,L)} + b\,||\eta^0||^2_{L^2(0,L)} + ||\xi^0||^2_{L^2(0,L)} \\ & + \sum_{n=0}^{N}\left(||\xi^{n+\frac{1}{2}}||^2_{L^2(0,L)} - ||\xi^n||^2_{L^2(0,L)}\right) \end{aligned}$$

Energy of the solution

Energy of A-operator:

$$\|\xi^{n+\frac{1}{2}}\|^2_{L^2(0,L)} \le \|\xi^n\|^2_{L^2(0,L)} + \|\boldsymbol{u}^n\|^2_{L^2(\Omega(t_n))} - \|\boldsymbol{u}^{n+1}\|^2_{L^2(\Omega(t_{n+1}))}$$
$$+ \quad 2c\Delta t|P_{in}^{n+1}|^2$$

Energy of B-operator:

$$\begin{aligned} & a\,\|\eta_{x_1}^{N+1}\|^2_{L^2(0,L)} + b\,\|\eta^{N+1}\|^2_{L^2(0,L)} + \|\xi^{N+1}\|^2_{L^2(0,L)} \\ = \quad & a\,\|\eta_{x_1}^{0}\|^2_{L^2(0,L)} + b\,\|\eta^{0}\|^2_{L^2(0,L)} + \|\xi^{0}\|^2_{L^2(0,L)} \\ & + \sum_{n=0}^{N}\left(\|\xi^{n+\frac{1}{2}}\|^2_{L^2(0,L)} - \|\xi^n\|^2_{L^2(0,L)}\right) \end{aligned}$$

Energy estimate of the solution:

$$E^{N+1} \le E^0 + \sum_{n=0}^{N} 2c\Delta t|P_{in}^{n+1}|^2$$

$$E^k = \|\boldsymbol{u}^k\|^2_{L^2(\Omega(t_k))} + a\,\|\eta_{x_1}^k\|^2_{L^2(0,L)} + b\,\|\eta^k\|^2_{L^2(0,L)} + \|\xi^k\|^2_{L^2(0,L)}$$

Outline

- ✔ *Wall Shear Stress*

$$WSS := \tau_w = -\mathbf{T}_f \boldsymbol{n} \cdot \boldsymbol{\tau}, \tag{1}$$

negative values of the WSS - indicate existence of large recirculation zones

- *Oscillatory Shear Index*

$$OSI := \frac{1}{2}\left(1 - \frac{\int_0^T \tau_w \, dt}{\int_0^T |\tau_w| \, dt}\right), \tag{2}$$

measures temporal oscillations of the shear stress pointwisely - indicates areas with large stenotic plug danger

- Reynolds number

$$RE_0 = \frac{\rho V l}{\mu_0} \quad \text{or} \quad RE_\infty = \frac{\rho V l}{\mu_\infty} \quad \text{or} \quad RE = \frac{\rho V l}{\frac{1}{2}(\mu_0 + \mu_\infty)}$$

- ✔ *Wall Shear Stress*

$$WSS := \tau_w = -\mathbf{T}_f \boldsymbol{n} \cdot \boldsymbol{\tau}, \tag{1}$$

negative values of the WSS - indicate existence of large recirculation zones

- ✔ *Oscillatory Shear Index*

$$OSI := \frac{1}{2}\left(1 - \frac{\int_0^T \tau_w \, dt}{\int_0^T |\tau_w| \, dt}\right), \tag{2}$$

measures temporal oscillations of the shear stress pointwisely - indicates areas with large stenotic plug danger

- Reynolds number

$$RE_0 = \frac{\rho V l}{\mu_0} \quad \text{or} \quad RE_\infty = \frac{\rho V l}{\mu_\infty} \quad \text{or} \quad RE = \frac{\rho V l}{\frac{1}{2}(\mu_0 + \mu_\infty)}$$

✔ *Wall Shear Stress*

$$WSS := \tau_w = -\mathbf{T}_f \boldsymbol{n} \cdot \boldsymbol{\tau}, \tag{1}$$

negative values of the WSS - indicate existence of large recirculation zones

✔ *Oscillatory Shear Index*

$$OSI := \frac{1}{2}\left(1 - \frac{\int_0^T \tau_w \, dt}{\int_0^T |\tau_w| \, dt}\right), \tag{2}$$

measures temporal oscillations of the shear stress pointwisely - indicates areas with large stenotic plug danger

✔ **Reynolds number**

$$RE_0 = \frac{\rho V l}{\mu_0} \quad \text{or} \quad RE_\infty = \frac{\rho V l}{\mu_\infty} \quad \text{or} \quad RE = \frac{\rho V l}{\frac{1}{2}(\mu_0 + \mu_\infty)}$$

Inflow data

inflow velocity

pulsatile parabolic profile

$$u_{inflow}(-L, x_2) = V(1 - x_2)(1 + x_2)\sin^2(\pi t/\omega) \quad on \quad \Gamma_{in},$$

or some $f(t)$, e.g.,illiac artery measurements

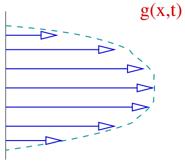

Inflow data

inflow velocity

pulsatile parabolic profile

$$u_{inflow}(-L, x_2) = V(1 - x_2)(1 + x_2)\sin^2\left(\pi t/\omega\right) \quad on \quad \Gamma_{in},$$

or some $f(t)$, e.g.,illiac artery measurements

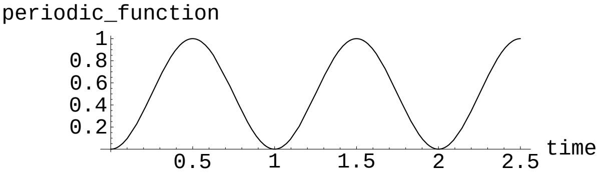

inflow velocity

pulsatile parabolic profile

$$u_{inflow}(-L, x_2) = V(1-x_2)(1+x_2)\sin^2(\pi t/\omega) \quad on \quad \Gamma_{in},$$

or some $f(t)$, e.g.,illiac artery measurements

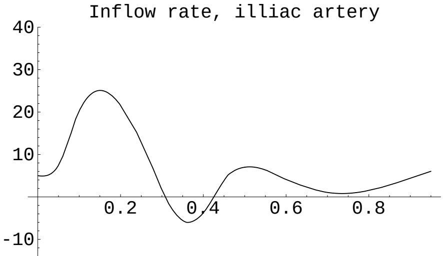

$$Q(t) = \int_{\Gamma_{in}} \boldsymbol{u}_{inflow} dx_2 \quad \Longrightarrow \quad f(t) = Q(t)\frac{3}{4VR(t)}$$

domain deformation: stenosed and straight channel

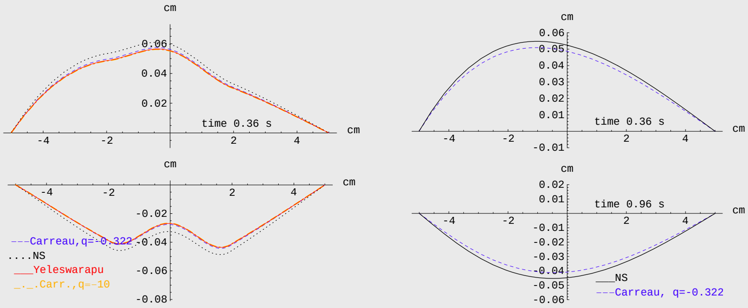

Some hemodynamical quantities

WSS-stenosed channel

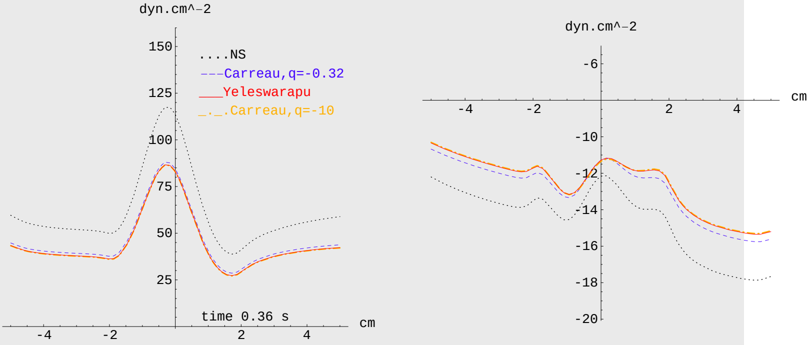

Some hemodynamical quantities

OSI

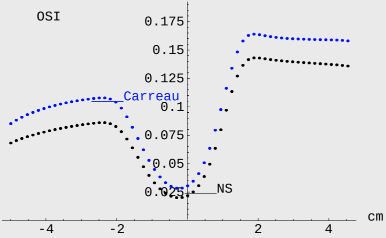

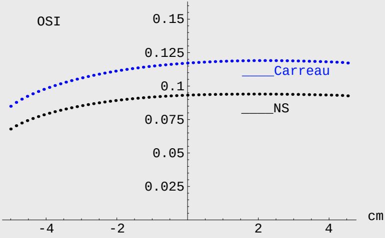

M.L. & A. Hundertmark [Comp.& Math.Appl. ('10)]

Outline

Summary

1. Effects due to complex geometry:
   wall deformation, extrema of WSS, OSI in stenosed / bifurcation regions
2. Effects due to the Non-Newtonian rheology:
   WSS: larger negative absolute value $\Longrightarrow$ recirculation zones,
   OSI: larger extremes $\Longrightarrow$ more sensible prediction of stenotic plug
3. Difference between Carreau and Yeleswarapu model:
   negligible

Summary

1. Effects due to complex geometry:
   wall deformation, extrema of WSS, OSI in stenosed / bifurcation regions
2. Effects due to the Non-Newtonian rheology:
   WSS: larger negative absolute value $\Longrightarrow$ recirculation zones,
   OSI: larger extremes $\Longrightarrow$ more sensible prediction of stenotic plug
3. Difference between Carreau and Yeleswarapu model:
   negligible
4. FSI & kinematical coupling: efficient, stable FSI algorithm